Enhanced Sensitivity of Zero-Field NMR Spectroscopy at High Magnetic Fields

H. Ernst[a], M. Fechtelkord[b], D. Fenzke[a], D. Freude[a], B. Knorr[a], H. Kolley[a], and H. Pfeifer[a]

[a] Universität Leipzig, Abteilung Grenzflächenphysik, Linnéstr. 5, D-04103 Leipzig
[b] Westfälische Wilhelms Universität, Inst. f. Phys. Chemie, Schloßplatz 4–7, D-48149 Münster

Z. Naturforsch. **50a**, 388–394 (1995); received December 24, 1995

Dedicated to Professor Müller-Warmuth on the occasion of his 65th birthday

After reviewing the basic principles of zero-field NMR spectroscopy at high magnetic fields (ZFHF NMR) as introduced by Robert Tycko, a 2-dimensional extension of this method is described which enhances its sensitivity by at least one order of magnitude. The essential point is a combination of the original pulse program including sample rotation with a Carr-Purcell pulse sequence during the acquisition time. Experimental results are given for the proton resonance of meta-$C_6H_2D_4$ dissolved in C_6D_6 at 245 K.

Key words: Zero-field NMR; High magnetic fields; 2-dimensional spectroscopy; Proton-proton distance; Benzene.

1. Introduction

The field of NMR has developed very rapidly during the last thirty years especially due to the invention of techniques that allow a measurement of highly resolved NMR spectra in solids. As is well known, the Hamiltonian H which determines the properties of a spin system can be written as

$$H = H_Z + H_d + H_{csa} + H_J + H_q + H_{rf}, \qquad (1)$$

where H_Z is the Zeeman interaction, including the isotropic chemical shift, between the nucleus and the applied static magnetic field B_0. H_d denotes the magnetic dipole interaction, H_{csa} the interaction due to chemical shift anisotropy, H_J the indirect electron-coupled nuclear spin interaction (J-coupling), H_q the electric quadrupole interaction which is only present for nuclei with spin $I \geq 1$, and H_{rf} the interaction with an alternating magnetic field, mostly applied in the form of short rf pulses.

In nonviscous liquids, H_d, H_{csa} and H_q average to zero so that highly-resolved NMR spectra can be observed containing the valuable information given by the isotropic values of the chemical shift and of the J-coupling. On this basis (fingerprint system) high-resolution nuclear magnetic resonance spectroscopy has become one of the most important tools in analytical chemistry. In the solid state, however, H_d, H_{csa}, and H_q are dominant, which leads to such a broadening of the NMR lines that in general the chemical shift of the lines and their splitting due to the J-coupling cannot be observed. To obtain highly resolved NMR spectra in solids, a selective removal of each of the broadening interactions is necessary. Generally, manipulations of spatial or spin variables of the Hamiltonian given in (1) can be performed. The new techniques of solid-state NMR, namely multiple pulse sequences, high-power dipolar decoupling, cross-polarization (CP), magic angle spinning (MAS) of the sample, combined rotation and multiple pulse sequence (CRAMPS), variable angle spinning (VAS), dynamic angle spinning (DAS) and double rotation (DOR) eliminate or at least reduce to a certain degree the influence of H_d, H_{csa}, and H_q, thus making possible the observation of one- and two-dimensional highly resolved NMR spectra in solids [1–3].

On the other hand H_d and H_q contain valuable information about the structure of the solid, viz. about intramolecular distances between nuclei (from H_d) and internal electric field gradients (fom H_q). However, when the material under study is not a single crystal so that all or many orientations of the local axes are present, the NMR spectra consist of strongly broadened "powder pattern" lines from which quantitative structure data can be derived only through a lineshape fitting procedure yielding values which are

Reprint requests to Dr. H. Ernst.

0932-0784 / 95 / 0400-0388 $ 06.00 © – Verlag der Zeitschrift für Naturforschung, D-72027 Tübingen

not very accurate. In zero field, the coupling can not depend on orientation because of the isotropy of space in the absence of external fields so that zero-field NMR spectra must exhibit sharp, well-resolved lines with splittings that contain the structural information. Therefore, even since the early days of NMR there has been considerable interest in the NMR spectra of solids in the absence of an external magnetic field [4–7]. Experimentally through the field cycling technique [8] zero-field NMR spectra can be observed in those cases where the spin-lattice relaxation time T_1 in low field is at least comparable to the time needed to complete a cycle which is typically greater than 100 ms. In contrast, the method introduced by Tycko [9] yields zero-field NMR spectra while maintaining the sample in the high field throughout the experiment (ZFHF NMR). The spectra are acquired by observing high field NMR signals while rapidly rotating the sample and applying specific sequences of resonant rf pulses in synchrony with the sample rotation. Therefore there is no limitation by short spin-lattice relaxation times, and moreover the isotopic selectivity of high field NMR is preserved.

In the present paper, an extension of this method is introduced which enhances the sensitivity by at least one order of magnitude. Experimental details of the new method are given and first results are presented for the ^{1}H ZFHF NMR spectrum of 4 m% meta-$C_6H_2D_4$ dissolved in 96 m% C_6D_6 at 245 K.

2. Theory of ZFHF NMR

2.1. General Principles

The Hamiltonian of the magnetic dipole interaction in the laboratory frame between two spins $\boldsymbol{I}_1$ and $\boldsymbol{I}_2$ with the same magnetogyric ratio γ (homonuclear interaction) and the internuclear vector $\boldsymbol{r}_{1,2}$ is given by

$$H_{\mathrm{d}}^{\mathrm{ZF}} = \frac{b_{1,2}}{3}\left(\frac{3}{r_{1,2}^2}(\boldsymbol{r}_{1,2}\boldsymbol{I}_1)(\boldsymbol{r}_{1,2}\boldsymbol{I}_2) - \boldsymbol{I}_1\boldsymbol{I}_2\right)$$

with

$$b_{1,2} = 3\frac{\mu_0}{4\pi}\frac{\gamma^2\hbar}{r_{1,2}^3}. \tag{2}$$

Introducing the angles ϑ' and φ' that specify the direction of the internuclear vector $\boldsymbol{r}_{1,2}$ in the laboratory axis system with the external magnetic field B_0 along the z-axis, the second-rank spherical harmonics $Y_{2,m}$ and the second-rank irreducible tensor operators $T_{2,m}$ (for definitions cf. [10]), (2) may be rewritten as

$$H_{\mathrm{d}}^{\mathrm{ZF}} = b_{1,2}\sum_{m=-2}^{2}(-1)^m Y_{2,m}(\vartheta',\varphi')\,T_{2,-m}. \tag{3}$$

In high field ($\gamma B_0 \gg b_{1,2}$) the only part on the right hand side of (3) that contributes to the NMR spectra is the so-called secular term

$$H_{\mathrm{d}} = b_{1,2}\,Y_{2,0}(\vartheta',\varphi')\,T_{2,0}. \tag{4}$$

Similar to (3), the Hamiltonian H_{c}, which includes the isotropic and anisotropic chemical shift, the resonance offset and heteronuclear magnetic dipole interaction as well, can be written as

$$H_{\mathrm{c}} = c_0\,T_{1,0} + \sum_{h=1}^{3} c_h\,Y_{2,0}(\vartheta_h',\varphi_h')\,T_{1,0}. \tag{5}$$

For the chemical shift $c_0 = \gamma B_0 \sigma_{\mathrm{iso}}$ and $c_h = (2/3)^{1/2}\gamma B_0 \sigma_h$, where σ_h ($h = 1,2,3$) are the principal values of the tensor of the chemical shift anisotropy and ϑ_h' and φ_h' describe the direction of the external magnetic field in the corresponding PAS. Under rotation of the sample around an axis inclined by the angle θ with respect to the external magnetic field, $Y_{2,0}(\vartheta',\varphi')$ can be expressed as a function of the angles ϑ and φ specifying the direction of the internuclear vector $\boldsymbol{r}_{1,2}$ in that system where the z-direction is given by the axis of rotation:

$$Y_{2,0}(\vartheta',\varphi') = \sum_{m=-2}^{2} d_{m,0}^{(2)}(\theta)\,e^{-im\omega_{\mathrm{rot}}t}\,Y_{2,m}(\vartheta,\varphi). \tag{6}$$

$d_{m,n}^{(L)}$ denote Wigner's reduced rotation matrices (for definitions cf. [10]). The Hamiltonian H_{rf} describing the interaction of the spins with the rf pulses is given in the frame rotating without offset with the Larmor frequency $\omega_0 = \gamma B_0$ by

$$H_{\mathrm{rf}} = \omega_1(t)(I_x\sin\alpha + I_y\cos\alpha), \tag{7}$$

where $\omega_1(t)$ and α denote, as usual, the amplitude and the phase of the rf pulses, respectively. In the interaction representation defined by H_{rf}, it follows for the Hamiltonians of (4) and (5) averaged over the cycle time T_{c} (average Hamiltonians),

$$\bar{H}_{\mathrm{d}} = b_{1,2}\sum_{n,m} f_{m,n}^{(2,2)}\,Y_{2,m}(\vartheta,\varphi)\,T_{2,n} \tag{8}$$

and

$$\bar{H}_{\mathrm{c}} = c_0\sum_{n} f_{0,n}^{(0,1)}\,T_{1,n} + \sum_{h} c_h \sum_{n,m} f_{m,n}^{(2,1)}\,Y_{2,m}(\vartheta_h,\varphi_h)\,T_{1,n}, \tag{9}$$

respectively. Here $f_{m,n}^{(K,L)}$ denote the scaling factors given by

$$f_{m,n}^{(K,L)} = \frac{1}{T_c} \int_0^{T_c} d_{m,0}^{(K)}(\theta)\, D_{n,0}^{(L)}(t)\, e^{-im\omega_{rot}t}\, dt \qquad (10)$$

with K = 0 or 2 and $L = 2$ or 1. $D_{n,m}^{(L)}(t)$ follows from the recursion formula

$$D_{n,m}^{(L)}(t + t_w) = \sum_{k=-L}^{L} D_{n,k}^{(L)}(t)\, e^{ik\alpha}\, d_{k,m}^{(L)}(\beta(t_w))\, e^{-im\alpha} \qquad (11)$$

with the rotation angle β as a function of the width of the rf pulse t_w

$$\beta(t_w) = \int_t^{t+t_w} \omega_1(t')\, dt' . \qquad (12)$$

The essential point of the theory of ZFHF NMR is to find conditions which make zero the average Hamiltonian of the isotropic chemical shift including a possible resonance offset ($f_{0,n}^{(0,1)} = 0$) and the anisotropy of the chemical shift, and therefore also of a heteronuclear magnetic dipole interaction ($f_{m,n}^{(2,1)} = 0$), while the average Hamiltonian of the homonuclear magnetic dipole interaction must be proportional to H_d^{ZF} as given by (2) ($f_{m,n}^{(2,2)} = \delta_{m,n} f e^{im\varkappa}$ with $\varkappa$ as an arbitrary real number and the Kronecker delta $\delta_{m,n}$). Summarized, the following conditions must be fulfilled:

$$\begin{aligned} f_{0,n}^{(0,1)} &= f_{m,n}^{(2,1)} = 0 , \\ f_{m,n}^{(2,2)} &= \delta_{m,n} f e^{im\varkappa} . \end{aligned} \qquad (13)$$

In order to simplify the treatment, four useful assumptions have been made [9]: (i) All pulses appear pairwise where the second rotates the spin in the opposite direction. (ii) One or more pulse pairs form a subcycle of duration T_{subc}. These subcycles are repeated with a phase increase of $2\pi/5$ or $-2\pi/5$ [11]. (iii) The duration of five subcycles ($5\,T_{subc}$) is equal to the period $2\pi/\omega_{rot}$ of the rotation of the sample. Therefore, we denote the sequence of five subcycles as a rotcycle. (iv) The cycle time T_c consists of N rotation periods of the sample ($T_c = 2\pi N/\omega_{rot}$). Under these suppositions (10) simplifies to

$$f_{m,n}^{(K,L)} = \frac{\delta_{m,n}}{T_{subc}} \int_0^{T_{subc}} d_{n,0}^{(K)}(\theta)\, d_{n,0}^{(L)}(\beta(t))\, e^{in(\alpha - \omega_{rot}t)}\, dt . \qquad (14)$$

2.2. *Ideal Pulses*

It is assumed that the width of the pulses is negligible with regard to the lengths of delays between them (δ-function approximation), so that a pulse sequence can be described completely by the phase α_i, rotation angle $\beta_i = \omega_1 t_{wi}$ and pulse delay τ_i, as shown schematically in Figure 1.

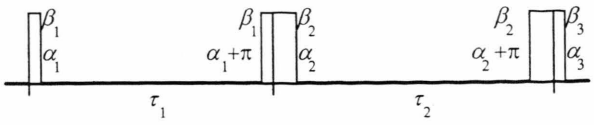

Fig. 1. Sequence of two pulse pairs in a subcycle. For ideal pulses their widths t_{wi} are negligible small with regard to their distances τ_i.

Assuming that a subcycle consists of S pulse pairs, (14) simplifies to

$$f_{m,n}^{(K,L)} = \frac{\delta_{m,n}}{T_{subc}} \sum_{s=1}^{S} d_{n,0}^{(K)}(\theta) \cdot d_{n,0}^{(L)}(\beta_s) \cdot \tau_s \frac{\sin(n\omega_{rot}\tau_s/2)}{n\omega_{rot}\tau_s/2} \cdot \exp(in\alpha_s') \qquad (15)$$

with

$$\alpha_s' = \alpha_s - \omega_{rot}(\tau_s + \tau_{s+1})/4 . \qquad (16)$$

For the special case $S = 2$ and $\theta = 75°$, which has been considered by Tycko [9], two rotcycles are necessary ($N = 2$) and two solutions exist in order to fulfill (13). The first is given by $\beta_1 = \beta_2 = \beta$, $\alpha_1 = 0$, $\alpha_2 = \alpha$, $\tau_1 = \tau_2 = T_{subc}/2$ and the condition that in the second rotcycle α must be exchanged with $-\alpha$ and moreover that it must be included in additional π pulses. The numerical results are collected in Table 1. The other solution is to use pulses of different rotation angles: $\beta_1 = \beta$, $\beta_2 = \pi - \beta$, $\alpha_1 = 0$, $\alpha_2 = \alpha$, $\tau_1 = \tau_2 = T_{subc}/2$ and the condition that in the second rotcycle α must be exchanged with $\alpha + \varepsilon$. For the results see also Table 1.

For $S = 4$ and $\theta = 75°$ only one rotcycle is necessary ($N = 1$). If we choose $\tau_1 = \tau_2 = \tau_3 = \tau_4 = T_{subc}/4$, a first solution is given by $\beta_1 = 45.790°$, $\beta_2 = 180° - \beta_1$, $\beta_3 = \beta_1$, $\beta_4 = \beta_2$, $\alpha_1 = 157.906°$, $\alpha_2 = 198°$, $\alpha_3 = \alpha_1$, $\alpha_4 = \alpha_1 + \alpha_2$, yielding $f = -0.08949$. As a second solution it can be found $\beta_1 = 67.283°$, $\beta_2 = 180° - \beta_1$, $\beta_3 = \beta_1$, $\beta_4 = \beta_2$, $\alpha_1 = 102.724$, $\alpha_2 = 198°$, $\alpha_3 = \alpha_1$, $\alpha_4 = \alpha_1 + \alpha_2$, yielding $f = +0.11039$. $N = 1$ means that a measurement can be performed after every rotation period, which enhances the accessible spectral region by a factor 2 compared with the former case ($N = 2$).

2.3. Real Pulses

Due to the finite pulse width and the time necessary for switching the phase between two pulses, the ideal-pulse sequence given in Fig. 1 has to be modified as follows: (i) The width of a pulse with a rotation angle β_i must be set to $t_{wi} = t_\pi \beta_i/\pi$ where t_π denotes the width of a pulse with $\beta = 180°$. (ii) Between two neighbouring pulses a pause of duration 2Δ must be inserted. Therefore, the ideal-pulse sequence of Fig. 1 leads to the pulse sequence shown in Fig. 2, for which the length of the sequence is also given by the rotation frequency: $\tau_1 + \tau_2 = T_{subc} = 1/5\,\nu_{rot}$.

For the above discussed ideal-pulse sequence with $\beta_1 = \beta$, $\beta_2 = \pi - \beta$ and $\alpha_1 = 0$, $\alpha_2 = \alpha$ (second solution in Table 1), the conditions given by (13) can be fulfilled exactly by optimizing the values α, $\beta_2 - \beta_1$, $\tau_1/\tau_2 \neq 1$, and $\beta_1 + \beta_2 \neq \pi$.

Small misadjustments of the pulses give rise to a residual broadening due to heteronuclear magnetic dipole coupling and anisotropy of the chemical shift, which can be removed by changing the sign of the rf phases and applying π pulses for each two rotcycles. The sequence for $S = 2$ is shown schematically in Fig. 3, where each rectangle represents one sequence of Figure 2.

Table 1. Numerical results for two pulse pairs per subcycle ($S = 2$), cf. Fig. 1, and two rotcycles per cycle ($N = 2$).

$\theta = 75°$	β	α	ε	f
1. Solution	45.993°	157.906°	–	−0.08949
	67.227°	102.724°	–	+0.10996
2. Solution	45.993°	216°	121.906°	−0.08949
	67.226°	216°	66.724°	+0.10996

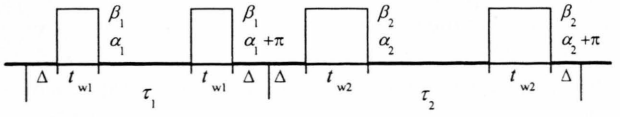

Fig. 2. Pulse sequence as in Fig. 1 but with a finite pulse width t_{wi} and a pause between the pulses.

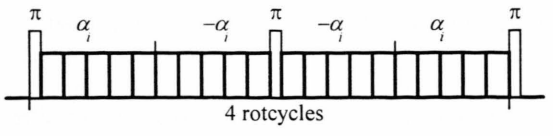

Fig. 3. The composed ZFHF pulse sequence.

3. Numerical Simulation

Three PC programs were developed (D. Fenzke). The first two allow a calculation of the scaling factor by means of (10) and an optimization of the rotation angles, phases, and distances of pulses for any real ZFHF pulse sequence. The third program can be used to simulate ZFHF NMR spectra for a given structure. As an example, the simulated ^{1}H ZFHF NMR spectrum of meta-$C_6H_2D_4$ shall be presented. The gyromagnetic ratio of spins 1 and 2 ($I = 1/2$) shall be denoted as γ_H, and that of the other spins ($I = 1$) as γ_D. This numbering of the ^{1}H nuclei (1, 2) must not be confound with the usual numbering in the benzene ring, which yields the positions 1 and 3 for ^{1}H in meta-$C_6H_2D_4$. The secular parts of the chemical shift anisotropy and of the magnetic dipole interactions were considered under the condition of a fast rotation of the molecule around its C6 axis. For the Hamiltonians introduced in (4) and (5) it follows

$$H_d = b_{12}(I_{1z}I_{2z} - \tfrac{1}{3}I_1 I_2)(3\cos^2\vartheta - 1)/2, \tag{17}$$

and

$$\begin{aligned} H_c = &+ \omega_0 \sigma_{iso}(I_{1z} + I_{2z}) \\ &+ \tfrac{1}{2}(3\cos^2\vartheta - 1)\{\omega_0 \tfrac{2}{3}\Delta\sigma(I_{1z} + I_{2z}) \\ &+ \tfrac{1}{3}\textstyle\sum_j (b_{1j}I_{1z} + \sum b_{2j}I_{2z})m_j\} \end{aligned} \tag{18}$$

with

$\Delta\sigma = \frac{1}{2}(2\sigma_3 - \sigma_1 - \sigma_2)$, $\sigma_{iso} = \frac{1}{3}(\sigma_3 + \sigma_1 + \sigma_2)$ and $m_j = \langle S_{jz}\rangle = \in(+1, 0, -1)$.

b_{ij} were introduced in analogy to (2), where γ^2 must be substituted by $\gamma_i\gamma_j$, and r_{12} by r_{ij}. In the I_z representation for the equivalent nuclei 1 and 2 the matrix of the Hamiltonian $H_d + H_c$ is given by

$$\begin{Vmatrix} -A+B & 0 & 0 & 0 \\ 0 & -A-B & 0 & 0 \\ 0 & 0 & 2A & C \\ 0 & 0 & C & 0 \end{Vmatrix} \tag{19}$$

with

$$A = -\tfrac{1}{12}b_{12}(3\cos^2\vartheta - 1)/2,$$

$$B = \omega_0\sigma_{iso} + (\tfrac{2}{3}\omega_0\Delta\sigma + \tfrac{1}{6}\textstyle\sum(b_{1j} + b_{2j})m_j)(3\cos^2\vartheta - 1)/2,$$

$$C = +\tfrac{1}{6}\textstyle\sum(b_{1j} - b_{2j})m_j(3\cos^2\vartheta - 1)/2.$$

The ^{1}H–^{1}H distance is $r_{12} = 0.429$ nm, and the ^{1}H–^{2}H distances to the nearest neighbours are

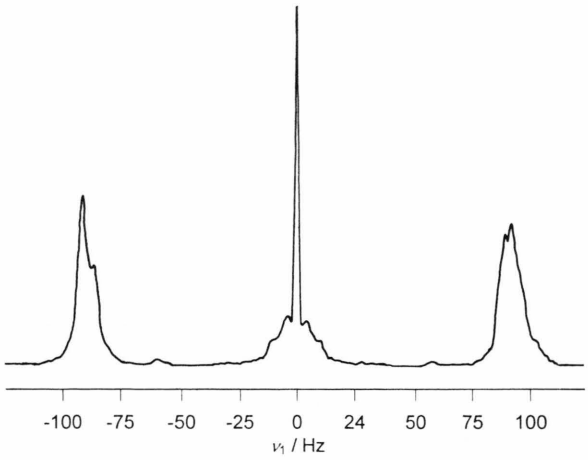

Fig. 4. Simulated ^{1}H ZFHF NMR spectrum of meta-benzene.

$r_{1j} = r_{2j} = 0.248$ nm (cf. [9]). The value of the anisotropy of the chemical shift $\Delta\sigma = 5.3$ ppm is taken from Ryan et al. [12]. The ZFHF spectrum calculated with these values is shown in Figure 4. The pulse sequence given in Fig. 2 was optimized for $\theta = 66°$, $\nu_{rot} = 3$ kHz, $t_\pi = 7$ μs, and $\Delta = 1.25$ μs. The obtained values are $\alpha = 161.43°$, $\beta_1 = 61.40°$, $\beta_2 = 149.35°$, $\tau_1/\tau_2 = 0.72$. The calculated scaling factor is $f = 0.076$.

4. Combined ZFHF and Carr-Purcell Pulse Sequence

In the original experiment of Tycko [9] after a preparation pulse ($\pi/2$) the sequence described in Figs. 2 and 3 is applied n times so that the evolution time of the spin system ($t_1 = n\,T_c$) can be increased in steps of T_c. The cycle time T_c corresponds to 4 rotation periods. The acquisition (running time t_2) of the NMR signal starts after the last rf pulse. Finally a two-dimensional Fourier transformation must be performed with respect to both the acquisition time t_2 and the evolution time t_1.

In the present work, a Carr-Purcell [13] pulse sequence with one synchronized π pulse per sample rotation is applied during the acquisition time t_2, and the amplitude of the NMR signal is measured between these pulses (see Figure 5).

Engelsberg et al. [14] have shown that the NMR spectrum of a homonuclear two-spin system measured by means of a Carr-Purcell pulse sequence consists of the superposition of a Pake doublet and a narrow signal in the centre. The latter is caused by a spin-lock term due to the combined action of H_d and H_c, cf. (4) and (5), under the influence of finite pulse widths. The zero-order Hamiltonian averaged over the cycle time of the Carr-Purcell pulse sequence $\overline{H_d + H_c}^{(0)}$ contains only the homonuclear dipolar interaction. However, the first-order approximation gives for a finite value of the pulse width t_π which has been assumed for simplicity to be much smaller than the pulse distance

$$\overline{H_d + H_c}^{(1)} = -\frac{\Delta\omega\, t_\pi}{\pi} b_{1,2}(I_{1x}I_{2z} + I_{1z}I_{2x}) + \frac{(\Delta\omega)^2 t_\pi}{\pi} I_{1x}. \tag{20}$$

In this expression the effects of resonance offset, chemical shift and heteronuclear magnetic dipole interaction are included in $\Delta\omega$. The second term in (20) causes the spin lock, which gives the narrow central signal with an intensity proportional to that of the doublet. It is the measurement of this narrow signal which increases the signal-to-noise ratio by more than one order of magnitude compared with the original ZFHF experiment.

5. Experimental

^{1}H NMR experiments were performed at a resonance frequency of 300 MHz using a spectrometer Bruker MSL 300 with a modified 7 mm MAS probe. The angle θ between the rotor axis and the external magnetic field was adjusted to $\theta = 66.0 \pm 0.1°$ by means of a laser beam. The latter could be calibrated by the probe axis ($\theta_1 = 0°$) and the magic-angle ($\theta_2 = 54.74°$), which was adjusted by a ^{81}Br MAS NMR experiment with a KBr sample. The Bruker MAS pneumatic control unit was used in combination with a temperature stabilization of the bearing gas nitrogen in order to obtain a rotational frequency of 3000 ± 2 Hz and a measuring temperature of 245 ± 1 K. Pulse durations and pulse phases were adjusted in channel 5 of the Bruker pulse programmer with a minimum duration of 2.5 μs, which could be increased in steps of 25 ns, and an accuracy of 1° for the phases. A vector volt meter HP 8508A was used for the initial calibration of the phases. The applied rotational frequency of 3 kHz results from the minimum pulse durations and distances which must be set in one cycle.

Spherical glass containers with an inner and outer diameter of 3 mm and 3.6 mm, respectively (with a

capillary on the top of 1.2 mm outer diameter and 5 mm length) were filled with the liquid substances and fused. Their symmetric position in the rotor was fixed by a capsule of the polymer PCTFE. In order to avoid inter-molecular proton-proton dipole interaction, 4 m% meta-$C_6H_2D_4$ were dissolved in fully deuterated (99.85%) benzene. The longitudinal relaxation time of the meta-benzene sample is about 20 s at 245 K. The strength of the rf field for a $\pi/2$ was adjusted with a water sample at room temperature and corrected at 245 K with an acetone sample. Various pulse sequences [15–17] were used for the final adjustment of rf phases, rf field strength, and tuning of the probe. After the adjustment of the optimized values given at the end of Chapter 3, the phase differences π and $\pi/2$ were set up.

In order to determine the inhomogeneity of the rf field strength B_1, a sequence of identical $\pi/2$ pulses was applied and the number n of pulses after which the free induction decreased to $1/e$ of its initial value was measured. Assuming a Gaussian distribution of the rf field strength B_1 in the sample, the standard deviation ΔB_1 can be determined by the equation

$$\frac{\Delta B_1}{B_1} \approx \frac{0.9}{n}. \tag{21}$$

Measurements with the water sample yielded an inhomogeneity of less than 2%.

The pulse sequence shown in Fig. 5 (details in Figs. 3 and 2) was used for the measurement of the meta-benzene. The scaling factor of the homonuclear magnetic dipole interaction is 0.076. Up to 32 cycles were applied and 32 or 64 scans were performed with a repetition time of 30 s.

6. Results and Discussion

Figure 6 presents the dependence of the spectra on the evolution time $t_1 = n T_c = n 4/\nu_{rot}$ for $n = 0-15$. Each of the 16 spectra (spectrum width 1.5 kHz) was obtained by a Fourier transformation of the Carr-Purcell NMR signals (running time t_2, see Fig. 5). It can be seen in this figure that the variation of the intensity of the doublet (peak distance of 800 Hz) is reflected in the variation of the intensity of the narrow line with a width of only 4 Hz.

If this narrow line is used instead of the doublet for the Fourier transformation with respect to the evolution time t_1, the signal-to-noise ratio increases by a

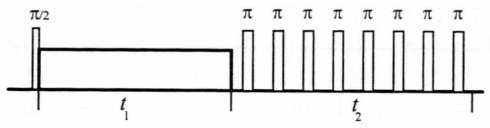

Fig. 5. Combined ZFHF and Carr-Purcell pulse sequence. n ZFHF cycles are applied during the time t_1. Each ZFHF cycle corresponds to that given in Figs. 3 for 4 rotcycles. One synchronized π pulse per sample rotation is applied during the time t_2.

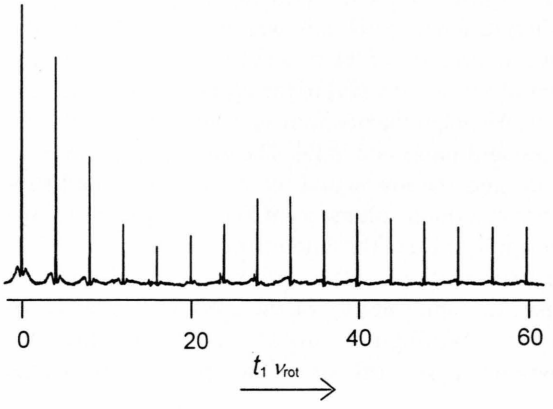

Fig. 6. Dependence of the spectra on the evolution time $t_1 = n T_c = n 4/\nu_{rot}$ for $n = 0-15$. Each of the 16 spectra (spectrum width 1.5 kHz) was obtained by a Fourier transformation of the Carr-Purcell NMR signals (running time $t_2 = 1024/\nu_{rot}$, see Figure 5).

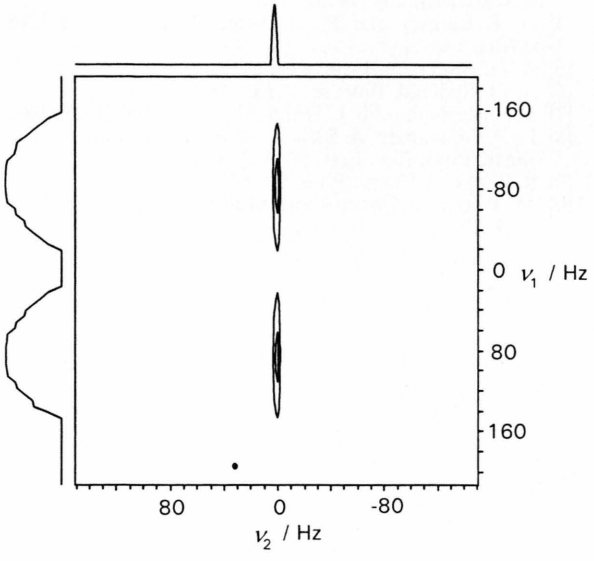

Fig. 7. Contour-plot of the two-dimensional ^{1}H ZFHF NMR spectrum of meta-benzene.

factor of 20. The obtained 2D ZFHF NMR spectrum of meta-benzene is shown in Figure 7. This spectrum does not contain the central line, which is generally obtained in zero-field spectra, since the spectrum taken after $n = 32$ was substracted from all other spectra before the t_1 Fourier transformation.

Figure 7 gives a splitting of 173 ± 3 Hz in good agreement with the value of 174 Hz obtained by Tycko [9]. Taking into consideration the value of the scaling factor ($f = 0.076$) it follows 0.429 ± 0.003 nm for the proton-proton distance in meta-$C_6H_2D_4$.

Only a few experiments were performed since the first presentation of the basic idea [18] and the experimental verification [19] of the ZFHF NMR spectroscopy. All experiments were carried out entirely by Tycko and published in [9]. The difficult experimental set-up and the low signal intensity of a diluted substance in a small volume seem to be the reasons for the rare application of this interesting method rather than the availability of suitable samples. With the present paper, the applicability of the method has been improved regarding both drawbacks. (i) The three PC programs developed allow an optimization of the pulse sequences with respect to the finite pulse length and the pauses between the pulses. (ii) By means of the application of a Carr-Purcell pulse sequence during the acquisition time t_2 an enhancement of the sensitivity of the method by at least one order of magnitude has been achieved: The spin lock resulting from the combined action of the homonuclear magnetic dipole interaction and chemical shift anisotropy and/or heteronuclear magnetic dipole interaction under the influence of finite pulse lengths gives rise to a narrow signal with an intensity proportional to that of the doublet, which was used for the measurements in the past.

Acknowledgement

The present paper is dedicated to Professor Werner Müller-Warmuth on the occasion of his 65th birthday. Moreover, the authors wish to express their gratitude to him for many stimulating discussions. Financial support by the Deutsche Forschungsgemeinschaft is gratefully acknowledged.

[1] M. Mehring, High Resolution NMR Spectroscopy in Solids, 2nd ed., Springer-Verlag, Berlin 1983.
[2] C. A. Fyfe, Solid State NMR for Chemists, C. F. C. Press, Guelph 1983.
[3] E. W. Wooten, K. T. Mueller, and A. Pines, Acc. Chem. Research **25,** 209 (1992).
[4] N. F. Ramsey and R. V. Pound, Phys. Rev. **81,** 278 (1951).
[5] A. G. Anderson, Phys. Rev. **115,** 863 (1959).
[6] A. G. Redfield, Phys. Rev. **130,** 589 (1963).
[7] R. E. Slusher and E. L. Hahn, Phys. Rev. **166,** 332 (1986).
[8] D. P. Weitekamp, A. Bielicki, D. B. Zax, W. Zilm, and A. Pines, Phys. Rev. Lett. **50,** 1807 (1983).
[9] R. Tycko, J. Chem. Phys. **92,** 5776 (1990).
[10] M. Weissbluth, Atoms and Molecules, Academic, New York 1978.
[11] B. F. Chmelka and A. Pines, Science **71,** 246 (1989).
[12] L. M. Ryan, R. C. Wilson, and B. C. Gerstein, J. Chem. Phys. **67,** 4310 (1977).
[13] H. Y. Carr and E. M. Purcell, Phys. Rev. **94,** 630 (1954).
[14] M. Engelsberg, C. S. Yannoni, M. A. Jacintha, and C. Dybowski, J. Amer. Chem. Soc. **114,** 8319 (1992).
[15] U. Haberlen, Magn. Reson. Rev. **10,** 81 (1985).
[16] D. P. Burum, M. Lindner, and R. R. Ernst, J. Magn. Reson. **43,** 463 (1981).
[17] U. Haubenreisser and B. Schnabel, J. Magn. Reson. **35,** 175 (1979).
[18] R. Tycko, J. Magn. Reson. **75,** 193 (1987).
[19] R. Tycko, Phys. Rev. Lett. **60,** 2734 (1988).